Neural Network LFM Pulse Compression

Jabran Akhtar
Norwegian Defence Research Establishment (FFI), Kjeller, Norway
Email: jabran.akhtar@ffi.no

***Abstract*—Matched filtering plays an important role in radar systems as the established pulse compression technique. This article puts forwards an alternative machine learning based technique for the matched filtering process assuming the incoming signal is oversampled. The aim is to replace the convolutional operation with a small fully connected feedforwarding neural network and attain an additional increase in the range resolution. The paper demonstrates how such a neural network design can be constructed and a practical training approach is presented. The results are compared against traditional matched filtering and target detection methods showing a clear advantage of trained neural networks for the pulse compression procedure and as a mean to construct inventive mismatched filters.**

***Keywords*—Radar, matched filter, mismatched filter, constant false alarm rate (CFAR), neural networks**

2023 IEEE Radar Conference (RadarConf23) | 978-1-6654-3669-4/23/$31.00 ©2023 IEEE | DOI: 10.1109/RADARCONF2351548.2023.10149646

I. Introduction

A wide variety of radar systems rely on matched filtering (MF) as an essential part of their signal processing chain. It is an optimal procedure for maximizing the signal to noise ratio (SNR) and with appropriate waveforms, such as linear frequency modulated (LFM) pulses, the resulting outcomes can be greatly compressed in range yielding high range resolution. In this regard, the bandwidth of the emit waveform plays an important factor as it determines the resolution in range and the ability to distinguish between closely spaced targets [1]. A wide bandwidth pulse is thus most preferable, however, this poses stringent requirements on the hardware alongside a large dedicated spectrum. Extended bandwidths may not always be available and some systems may also prefer to utilize smaller bandwidths in order to reduce their exposure and perhaps randomly hop between different carrier frequencies.

Recent years have also seen great increase in the application of machine learning methods, particularly deep neural networks, for e.g. target detection and classification. Deep learning techniques have been proposed as alternative to traditional reconstruction processes to obtain super-resolution images [2], [3], [4]. Even though the MF procedure is an optimal solution with respect to maximizing the SNR, there are many circumstances where other techniques can be seen as more beneficial. These approaches include mismatched filtering or least-square estimation methods who can be utilized to, for example, obtain greater control over the sidelobe levels at the expense of other properties such a lower peak gain [5], [6], [7], [8], [9], [10]. In theory, neural networks could be implemented to perform mismatched filtering with respect to specific conditions. The networks could be trained to approximate different outcomes with emphasis on for example sidelobe levels or greater range resolution while simultaneously taking into account the expected noise factor and distribution.

In a previous work [11] it was shown that the Doppler resolution of range-Doppler maps can be modestly incremented by neural networks. This was based solely on the application of the Fourier transform over a coherent processing interval and did not consider the range resolution which is determined by the properties of the pulse and the pulse compression procedure. The objective herein is to present a new time domain framework for the MF process and to demonstrate how appropriately trained neural networks (NN) can successfully provide a viable alternative with regard to traditional pulse compression and mismatched filtering. More specifically, we establish how oversampled radar signals can be evaluated through NN to obtain a high range resolution by seeking to approximate wider bandwidth pulses. The application of modern neural networks for pulse compression has till now not been given consideration in the available literature. A central contribution of the paper is further linked with demonstrating how NNs can be assembled to operate directly on raw complex data as input.

The method presented here is based on processing of incoming signals bin by bin but through a neural network, analogous to how a traditional discrete convolutional procedure in time-domain would be executed. This allows for flexibility as the standard MF process may be replaced by a neural network only where specific high resolution results are desired. The emphasis on small fully connected feedforwarding only neural networks demands low computational complexity once the network has been trained also permitting parallel execution over different range bins. A corresponding frequency domain processing is discussed in [12]. Waveform design and processing is normally not associated with particulars such as the noise floor level, however, a neural network can be trained to take account of these factors for specific optimization. To this end, a generic neural network design and training procedure is presented which may easily be adapted for different radar setups. Detailed simulation results are shown and are complemented by constant false alarm rate (CFAR) [13] target detection tests portraying detectional improvement with the implementation of a neural network instead of traditional MF processing.

II. System design

In this text we assume a standard radar model where a LFM pulse is transmitted with a given interval. The pulse may be defined as

$$p(t) = \exp\left(j2\pi(f_0 - \frac{\Delta f}{2})t + \frac{\Delta f}{2T}t^2\right), \tag{1}$$

where f_0 is the carrier frequency and Δf is the bandwidth. The pulse starts at $t = 0$ and terminates at $t = T$. The receiving signal containing N target reflections can therefore

be described as

$$s(t) = \sum_{l=1}^{N} \rho_n p(t - \Delta_n) e^{j2\pi\nu_l(t-\Delta_n)} + z(t) \tag{2}$$

where Δ_n corresponds to the delay of reflector l, ρ_n are complex-valued reflection coefficients, ν_l corresponds to frequency shift due to target velocity and $z(t)$ is white Gaussian noise. The radar has a maximum range up to r_{max} and the incoming data is collected with R number of samples in $s[n], 1 <= n <= R$. The discrete emitted pulse $p[n]$ is assumed to consist of L samples and, for simplicity, we ignore the aspects behind downsampling and baseband conversion. The sampling rate of the radar system is given by f_s and is set to satisfy the sampling theorem

$$f_s > 2\Delta f. \tag{3}$$

This rate may be significantly greater than the required minimum as oversampling is often utilized in radars. The range resolution of a pulse compression system is still determined by the bandwidth of the sent pulse, $\Delta R = \frac{c}{2\Delta f}$ where c is the speed of propagation.

In traditional processing, a matched filtering operation is assumed carried out on the receiving data using the time-reversed and conjugated discrete version of the sent pulse, i.e. $p^*[n]$. The matched filtering pulse may optionally be tapered with a windowing function to control the sidelobes [14], [15] and is thus denoted by $p_w^*[n]$. In order to deal satisfactory with different target velocities a bank of matched filters is frequently employed where different filters are aligned with respect to different Doppler values. In the following, but without loss of generality, we will assume that only a single filter of the bank is considered for $\nu_l = 0$. The described process may readily be iterated to construct a bank of networks tailored towards different Doppler values. The standard MF procedure can thus be specified as

$$y[n] = \sum_{m=L+1}^{R} s[m] p_w^*[n - m]. \tag{4}$$

In the above, the first L samples of the signal $s[n]$ are ignored but one may expand the signal by zero-padding or extrapolating using different techniques [15]. The procedure may be expressed through the use of the operator function

$$r[n] : s[n - L : n] \rightarrow y[n] \tag{5}$$

for $L + 1 \leq n \leq R$. The operator takes L preceding samples accompanying bin n and returns the matched filtered value for bin n.

To improve range resolution of this system, the transmission of a higher bandwidth pulse would ordinarily be required. To model an identical system, yet with higher bandwidth, an alternative version of the radar setup can be formulated where the employed pulse is replaced by

$$\hat{p}(t) = \exp\left(j2\pi(f_0 - \frac{\Delta\hat{f}}{2})t + \frac{\Delta\hat{f}}{2T}t^2\right), \tag{6}$$

where $\Delta\hat{f} > \Delta f$; however, where the sampling rate of the system still satisfies

$$f_s > 2\Delta\hat{f}. \tag{7}$$

The equivalent matched filtered output can be specified as

$$\hat{y}[n] = \sum_{m=L+1}^{R-L} \hat{s}[m] \hat{p}_w^*[n - m]. \tag{8}$$

This can also be instituted as a complex function

$$\hat{r}[n] : \hat{s}[n - L : n] \rightarrow \hat{y}[n] \tag{9}$$

where $\hat{p}_w^*[n]$ is the discrete conjugated and time-reversed higher bandwidth pulse with an optionally applied apodization function. Assuming that the radar transmits standard bandwidth pulses $p(t)$, but with a larger receiver sampling rate, the receiver output processing can hypothetically be adjusted to simulate the emission of a pulse with greater range resolution. This can be viewed as mismatched filtering where the objective is no longer SNR maximization but providing a modified matched filter output.

As per the description above, a new mapping can be proposed

$$r_{NN}[n] : s[n - L : n] \rightarrow \dot{y}[n] \tag{10}$$

where the sampled input data based on the lower bandwidth pulse $p(t)$ is utilized and an output $\dot{y}$,

$$\dot{y}[n] \approx \hat{y}[n], \;\; L + 1 \leq n \leq R, \tag{11}$$

is generated approximating the higher bandwidth pulse. This concept is deemed plausible as 1) the signal, $s[n]$, is assumed oversampled and 2) $\hat{y}[n]$ originates from a well established pulse compression procedure. In case of $\hat{p}[n] = p[n]$, the identify $\hat{y}[n] = y[n]$ is formed whereby the solution $\dot{y}[n]$ should ideally also converge to standard matched filtering. To determine $r_{NN}[n]$ one can initiate from the assumption that a set of M input and output training signals with both pulses are available, i.e.

$$s_1[n], \; s_2[n], ..., s_M[n] \Leftrightarrow y_1[n], \; y_2[n], ..., y_M[n] \tag{12}$$

and

$$\hat{s}_1[n], \; \hat{s}_2[n], ..., \hat{s}_M[n] \Leftrightarrow \hat{y}_1[n], \; \hat{y}_2[n], ..., \hat{y}_M[n]. \tag{13}$$

Every signal contains a number of targets arbitrary placed in range with random reflection values and random phase shifts. The frequency shift of the targets is also to be aligned with the Doppler shifts this neural network should be aimed for. The targets parameters are to be identical between $s_l[n]$ and $\hat{s}_l[n]$ for a given l, $1 \leq l \leq M$. Random placement of targets will inadvertently cause situations where multiple targets end up being close to each others and training on these scenarios thus also forces the network to learn the linearity of the system. In order to establish $r_{NN}[n]$ one can take advantage of modern neural networks as these networks are capable of approximating a wide variety of arbitrary functions. To formally construct the link

$$s_1[n], \; s_2[n], ..., s_M[n] \Rightarrow \dot{y}_1[n], \; \dot{y}_2[n], ..., \dot{y}_M[n] \tag{14}$$

through $r_{NN}[n]$ a machine learning training process can thus be initiated to minimize the mean square error:

$$r_{NN}[n] = \arg\min_{\dot{r}_{NN}} \sum_{l, \, n} ||\dot{r}_{NN}[n] - \hat{y}_l[n]||^2. \tag{15}$$

The error summation to be run across the entire data $1 \leq l \leq M, \; L + 1 \leq n \leq R$, or alternatively, a randomly determined

subset. The optimization above is not to be limited to signals containing target elements but will also include samples with only noise in them. The aim will be to return processed noise as filtered through high resolution MF assuming $z(t)$ is identical under both $p(t)$ and $\hat{p}(t)$. Normally, the construction of waveforms and the matched filter outcomes are not evaluated with respect to an expected noise and SNR level. In practice, one can argue that for low SNR targets high sidelobes after processing are not necessarily an issue if they remain below the noise floor. If the signaling scenario is not too diverse then the network training can be restrained for greater specialization.

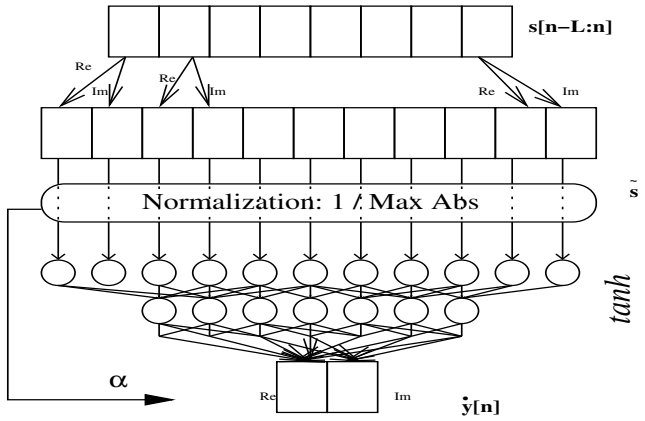

Fig. 1: Design of the network structure

A. Neural network design

The input $\mathbf{s} = s[n-L:n]$ and output $\dot{y}[n]$ of the neural network are complex valued and fully connected feedforwarding neural networks, with minor modifications as described in [11], can be utilized. Notably, the design

- splits complex data in real and imaginary parts treating them as separate entities
- makes use of maximum absolute normalization.

The input to the first layer of the neural network can subsequently be defined as a vector

$$\tilde{\mathbf{s}} = \frac{1}{\alpha}[\Re(\mathbf{s})\ \Im(\mathbf{s})] \ \in \mathbb{R}^{2L} \tag{16}$$

where

$$\alpha = \max\big(\ |\Re(\mathbf{s})|,\ |\Im(\mathbf{s})|\ \big), \tag{17}$$

i.e. the maximum absolute value of either the real or imaginary elements of $\mathbf{s}$. The largest absolute value of any of the inputs to the neural network will thus always be equal to one, while the lowest figure remains undefined. The output from the network will consist of two entries who are combined together to form a single complex value and scaled up by factor α. These two steps can be treated most easily outside the neural network. It turns out that maximum absolute normalization plays a key role for successful training of the network and accurate signal reconstruction. The number of nodes in each network layer and the number of layers can be adjusted to reflect the length of the input signal. A network containing only two output nodes of linear activation functions without any hidden layers will lead to a least square solution. It turns out that even networks with one or two hidden layers can yield very acceptable performance surpassing the least square outcomes, as will be analyzed in the next section. A sketch of the neural network design is given in figure 1. Notice that this model does not require the incorporation of any convolutional layers.

Parameter	
Pulse duration (bins)	$L = 128$
Sampling rate	$f_s = 25$kHz
Bandwidth $p(t)$	$\Delta f = 7$kHz
Bandwidth $\hat{p}(t)$	$\Delta \hat{f} = 12$kHz

TABLE I: Simulated baseband radar parameters

III. Simulated examples

This section demonstrates the laid out principles on some concrete examples and provides detailed simulation results. The examples are founded upon a baseband modeled radar, $f_0 = 0$, using a long duration pulse; with the main radar parameters as given in table I. The radar setup aims for a bandwidth expansion of 5kHz and attempts to maximize the range resolution up to the limit determined by the sampling rate. Each pulse reflection set to cover $L = 128$ range bins, equivalently $T = 0.0051s$. From reflections based on $\mathbf{p}$, the networks must produce an output resembling the application of $\hat{\mathbf{p}}$ after matched filtering. For reference, figure 2 displays the real and imaginary parts of the two waveforms with blue curve representing the standard bandwidth pulse of 7kHz and red the higher bandwidth pulse. All pulses have identical norm and for matched filtering all pulses are assumed tapered with the Hamming window.

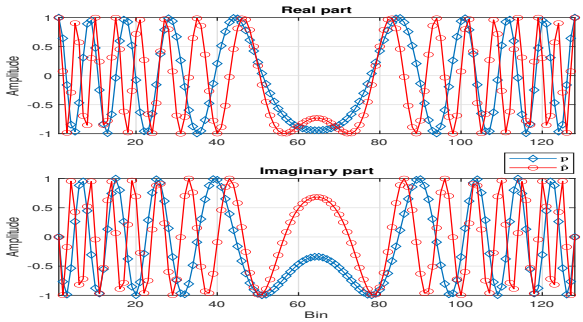

Fig. 2: Real and imaginary parts of simulated waveforms.

To evaluate the performance of neural networks we consider two different configurations:

- Z1: a NN with no hidden layers but two output nodes with linear activation functions
- N1: a NN with one hidden layers of 256 nodes ($tanh$ activation functions) and an output layer with linear activation functions

The network Z1 will illustrate the outcomes with a comparable least square solution. The second network N1 introduces hidden layers and should be able to construct more intricate mappings between the input and output. To train these networks a database of signals was generated with randomly selected, either two or three targets, with random reflection values selected from a Swerling 1 distribution with a mean

value of 0.25 and random phase shifts. The radar was set to cover a simulated range of $R = 600$ bins and positions of the targets was determined arbitrary, within the interval $[L, 600-L]$. Two different sets of networks were trained where each signal realization had a random noise floor selected from a given uniform distribution:

- set A: noise floor region between -80dB to -6dB
- set B: noise floor region between 6dB to 8dB.

The first set has a large noise variability and may experience many targets with large SNRs while the second set gives conditions for a more precisely defined radar setup where excessive noise plays a dominant which, on average, will result in a lower SNR regime. Conventionally, pulse design and MF is not linked with the noise floor which is what set A training is geared towards, however, the neural network processing step can be instituted to take account of radar specific parameters to optimize the results. The sidelobe levels can then be adapted by a NN to values just below the designated noise floor level. For training, from each set, random samples were collected and new signals generated until a training database totaling 1 million entries was complete. A visual example of a possible training signal is provided later in figure 8. The full data was employed to train fully connected neural networks using the scaled conjugate algorithm over 500000 epochs.

A. *Delay-Doppler characterization*

Radar pulses and corresponding filters are often characterized using the ambiguity function to evaluate their performance as a target exhibits shifts in Doppler and range. Processing the signals through neural networks will alter these basic properties and, as previously discussed, the networks should be trained corresponding to different targets velocities for inclusion in a filter bank. Figure 3 shows the delay-Doppler plot of the original waveforms using traditional MF. Employing the high resolution waveform (lower image) results in a narrower mainlobe and lower sidelobes. Figures 4 and 5 display the equivalent Z1 and N1 solutions where the trained networks now process signals consisting of the low bandwidth waveform $\mathbf{p}$. Notice that the diagrams incorporate the noise floor region of interest which the networks have been trained for. The solutions for set A in figure 4 show narrow mainlobes for both Z1 (top plot) and N1 (lower plot), however, the Z1 outcome contains noticeable sidelobes; in contrast, the N1 network demonstrates lower sidelobes, notably at Doppler velocities around 0 which is the main region for this filter. The same networks trained for a higher noise level in figure 4 show a markedly different picture. Although the mainlobes are still quite narrow, the least-square Z1 solution has a very large spread of sidelobes and a low peak gain. N1, on the other hand, manages to suppress the sidelobes greatly resulting in varying gain as a function of target velocity.

The curves corresponding to the zero Doppler curve can be seen in figures 6 and 7. To numerically quantify these plots, tables II and III can be consulted. The second column in table II is defined as $||n_p - n_{MF}||/||n_{MF}||$ which gives the relative error for zero Doppler curves between the selected pulse/network (n_p) of column one and the high bandwidth pulse (n_{MF}). PSL gives the peak sidelobe level while ISL refers to the integrated sidelobe level [1]. The half-power

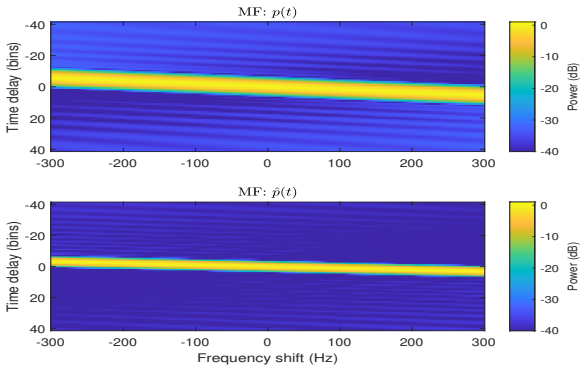

Fig. 3: Delay-Doppler diagram of MF with $\mathbf{p}$ and $\hat{\mathbf{p}}$.

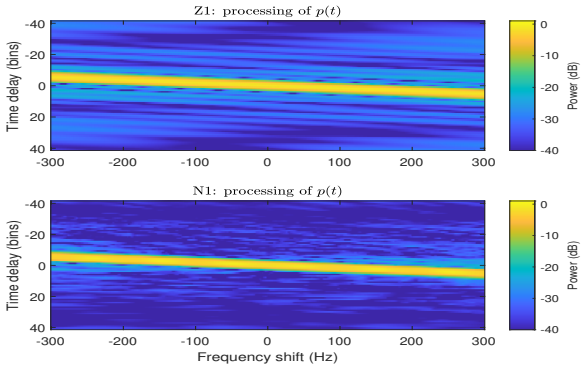

Fig. 4: Set A: Delay-Doppler diagram Z1 and N1.

width is given in number of range bins approximated using spline interpolation. It would be unrealistic to expect a perfect agreement from the N1 solutions towards $\hat{p}(t)$, however, N1 generally improves on the least square Z1 solutions with better fitting to the high resolution curve and reduces the original 3dB width significantly. The NN processing results in either lower ISL or PSL, or both; leading to a different compromise between the values of $p(t)$ and $\hat{p}(t)$. One can particularly comment that the NN network for set B in figure 7 exhibits a higher noise floor and two prominent sidelobes, however, the sidelobes are around 8 dB lower than the peak value being close to the noise floor level this network was trained for. The network can therefore still be expected to provide satisfactory

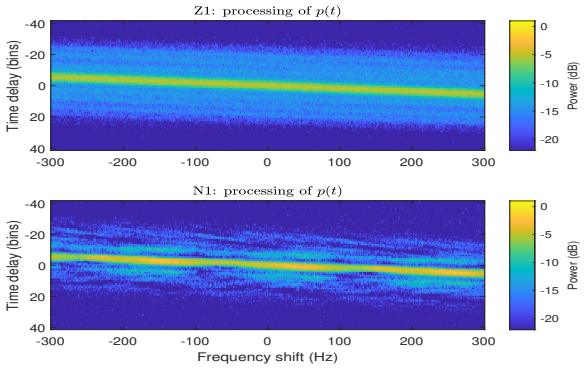

Fig. 5: Set B: Delay-Doppler diagram Z1 and N1.

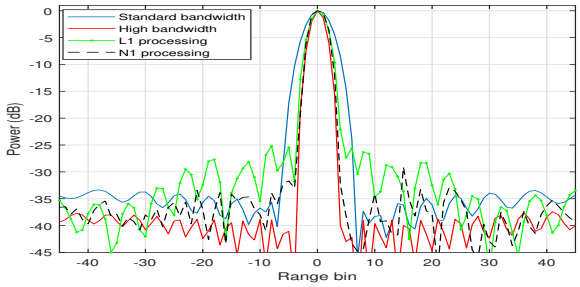

Fig. 6: Set A: zero-Doppler cut

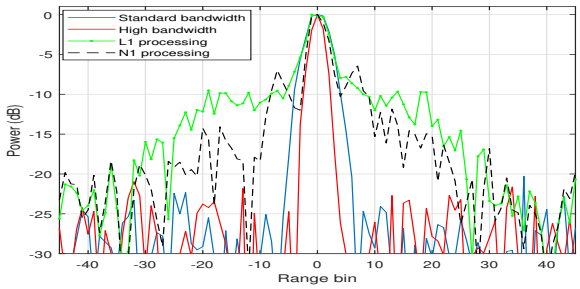

Fig. 7: Set B: zero-Doppler cut

outcomes in backgrounds it has been trained for.

Network	Relative error	PSL (dB)	ISL (dB)	3dB width (bins)
$p(t)$	0.5582	-33.35	-22.63	4.70
$\hat{p}(t)$	0	-37.42	-24.56	2.79
Z1	0.2182	-25.73	-17.27	3.40
N1	0.1560	-28.81	-20.42	3.34

TABLE II: Set A: Comparative values at zero Doppler

Network	Relative error	PSL (dB)	ISL (dB)	3dB width (bins)
$p(t)$	0.6506	-20.27	-10.74	4.70
$\hat{p}(t)$	0	-20.96	-9.57	2.79
Z1	1.2678	-7.82	1.17	4.18
N1	0.9784	-6.42	-0.44	3.63

TABLE III: Set B: Comparative values at zero Doppler

B. Single pulse evaluation

The delay-Doppler diagrams display some important properties of neural network against classical pulse compression, however, in a radar context the detectional aspects are crucial where the ability to separate closely spaced targets plays an important role. Radars mostly operate with known defined parameters, including e.g. noise figures, and the results given hereafter are based on set B settings. Figure 8 presents a visual example of a simulated signal with multiple targets, marked with a cross at top, stationed close to each others with increasingly distance and randomly chosen reflection values. The blue curve shows the magnitude outcome of matched filtering with $\mathbf{p}$ while the red line demonstrates the transmission and reception with $\hat{\mathbf{p}}$. The black dotted curve demonstrates the output from the trained N1 neural network operating on the low bandwidth signal. The outcome from the neural network closely matches the red higher bandwidth matched filtering with very identical narrow mainlobes for most of the targets. This is particularly the case for targets without neighbors. There are a few instances, such as range bins 310 and 325 where targets achieve a lower SNR gain with NN than would be the case with the original waveforms, but on the other side the targets at range bin 280 and 305 show an improvement over the original bandwidth pulse. The weak target at bin 300 is not detectable with the low bandwidth waveform which remains the case with the NN as well as. We also note the presence of stronger sidelobes at range bin 285 and 295. When it comes to noise only region, as can be seen on the left side of the plot, the network approximates the high resolution outcomes closely.

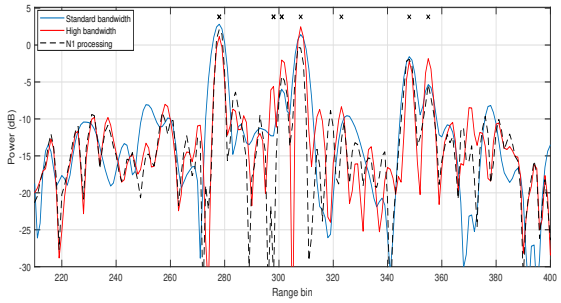

Fig. 8: Magnitude: MF and NN processing.

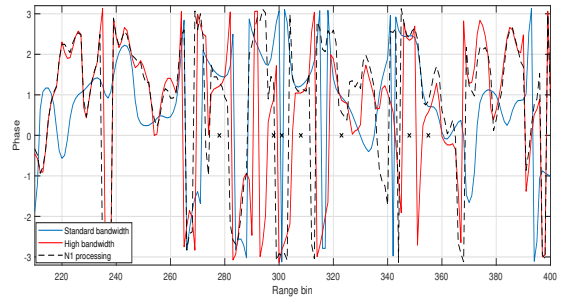

Fig. 9: Phase: MF and NN processing.

For coherent processing it is further important that the phase of the processed signal remains preserved; the phase of this signal can be seen in figure 9 where the phase values all converge at target locations, indicated by crosses at zero Doppler.

C. CFAR detection

The previous sections have discussed the basic aspects of incoming signals being processed with trained neural networks. The main disadvantages of NNs can be related to potential SNR loss and stronger sidelobes, this is though variable depending on e.g. targets strength and overlap. On the positive side the networks yield good approximation to high bandwidth pulses with narrower mainlobes and increased ability to separate targets. Some targets may also witness a slight improvement in the overall gain.

To quantify the benefits in a radar detectional context comprehensive simulations needs to be performed and to this end, cell averaging (CA) - CFAR detection tests were evaluated on low and high bandwidth signals alongside low bandwidth signals processed via trained neural network. The simulation scenario was set to be similar to figure 8 where

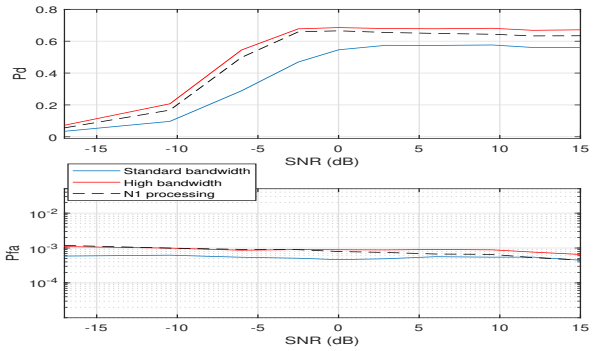

Fig. 10: Target detection, CFAR threshold 12dB

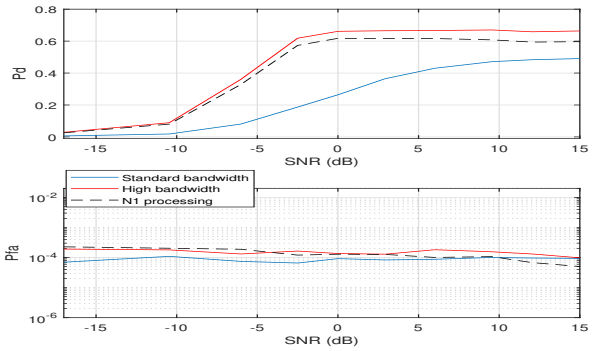

Fig. 11: Target detection, CFAR threshold 14dB

10 targets were positioned randomly across the range bins with reflection values set accordingly to a given SNR. Due to arbitrary placement many targets will end up being close to each others and a narrow mainlobe is essential to distinguish targets and obtain high detectional capability. The arbitrary target positioning and density makes it impossible to detect all targets even at high SNRs. For each SNR level 100000 simulations were carried out to determine the probability of detection (Pd) and the false alarm rate (Pfa) over a single pulse. The CA-CFAR parameters were set as 3 guard cells and 5 averaging cells on each side of cell under test (CUT) and detection thresholds of 12dB and 14dB. The CFAR tests in figures 10 and 11 with the N1 network (black dotted curve) offer a detection performance which is a bit lower than what would be achievable under the high resolution pulse (red curve) but is clearly beneficial compared to traditional MF (blue curve) on base waveform. The neural network approach further on retains the original false alarm rate. Overall, CFAR test evaluation shows an improvement with the application of neural network for target detectional purposes.

As a final note we remark that the network training and minimization formed by (15) forces a compromise between properties such as the widths and peak values of the mainlobe and the sidelobes alongside more inherent aspects such as system's linearity, the expected noise distribution and so forth. Some of these properties may be taken for granted in standard convolutional setting but may require explicit training in a neural network. By appropriately adjusting target parameters, Doppler constrains, noise floor and other environmental factors networks can be trained for specific scenarios with emphasis on select properties.

IV. Conclusion

The paper presented an alternative time domain convolutional approach based on neural networks for the pulse compression procedure. The networks were specifically designed and trained to yield an output approximating the utilization of a high bandwidth pulse taking account of radar specific parameters and assuming the incoming signals are oversampled. This provides an alternative method for the construction of mismatched filters where minor losses in e.g. peak gain may be traded for higher resolution. It was demonstrated that small fully connected feedforwarding neural networks can be trained for this purpose resulting in increased ability to detect closely spaced targets.

References

[1] N. Levanon and E. Mozeson, *"Radar Signals"*. New Jersey: Wiley, 2004.

[2] W. Yang, X. Zhang, Y. Tian, W. Wang, J.-H. Xue, and Q. Liao, "Deep learning for single image super-resolution: A brief review," *IEEE Transactions on Multimedia*, vol. 21, no. 12, Dec. 2019.

[3] J. Gao, B. Deng, Y. Qin, H. Wang, and X. Li, "Enhanced radar imaging using a complex-valued convolutional neural network," *IEEE Geoscience and Remote Sensing Letters*, vol. 16, no. 1, pp. 35–39, Jan. 2019.

[4] L. Lin, J. Li, Q. Yuan, and H. Shen, "Polarimetric SAR image super-resolution via deep convolutional neural network," in *IEEE International Symposium on Geoscience and Remote Sensing*, 2019, pp. 3205–3208.

[5] M. H. Ackroyd and F. Ghani, "Optimum mismatched filters for sidelobe suppression," *IEEE Trans. Aerospace and Electronic Systems*, vol. 9, no. 2, pp. 214–218, March 1973.

[6] S. D. Blunt, K. Gerlach, and T. Higgins, "Aspects of radar range super-resolution," in *IEEE Radar Conference*, 2007, pp. 683–687.

[7] L. Harnett, D. Hemmingsen, P. McCormick, S. Blunt, C. Allen, A. Martone, K. Sherbondy, and D. Wikner, "Optimal and adaptive mismatch filtering for stretch processing," in *IEEE Radar Conference*, 2018.

[8] J. Kempf and J. A. Jackson, "A modified least-squares mismatched filter for use in radar applications with additive noise," in *IEEE Radar Conference*, 2020, pp. 804–809.

[9] A. V. Delgado, M. Sánchez-Fernández, L. Venturino, and A. Tulino, "Super-resolution in automotive pulse radars," *IEEE J. Sel. Areas Comm.*, vol. 15, no. 4, pp. 913–926, June 2021.

[10] M. Coutino, F. Uysal, and L. Anitori, "Waveform-aware optimal window function design for mismatched filtering," in *IEEE Radar Conference*, 2022.

[11] J. Akhtar, "Augmenting radar Doppler resolution with neural networks," in *European Signal Processing Conference*, 2021, pp. 1551–1555.

[12] ——, "High-resolution neural network processing of LFM radar pulses," in *IEEE International Conference on Acoustics, Speech and Signal Processing*, 2023.

[13] P. P. Gandhi and S. A. Kassam, "Optimality of the cell averaging CFAR detector," *IEEE Trans. Inf. Theory*, vol. 40, no. 4, pp. 1226–1228, Nov. 1994.

[14] F. J. Harris, "On the use of windows for harmonic analysis with the discrete Fourier transform," *Proceedings of the IEEE*, vol. 66, no. 1, pp. 51–83, Jan. 1978.

[15] A. V. Oppenheim and R. W. Schafer, *"Discrete-Time Signal Processing"*. Prentice-Hall, 1989.